Int J Adv Manuf Technol (2012) 59:201–212
DOI 10.1007/s00170-011-3500-6

ORIGINAL ARTICLE

Jetting stability of molten caprolactam in an additive inkjet manufacturing process

Saeed Fathi · Phill Dickens · Richard Hague

Received: 27 February 2011 / Accepted: 26 June 2011 / Published online: 10 July 2011

Abstract This paper proposes a novel additive manufacturing concept which uses inkjet technology to manufacture parts in nylon 6. The methodology involved a series of experiments to investigate whether caprolactam, the monomer of nylon 6, could be jetted in the molten state. Once this was established, further experiments were undertaken to determine the possible boundaries for the process parameters. The main parameters were the vacuum level at which the melt could be controlled for stable jetting, the jetting voltage amplitude and frequency which were investigated against the jet array stability by monitoring the printhead's nozzle plate. The jet(s) instability behaviour were characterised in different sets of experiments in order to optimise the jetting conditions for the molten caprolactam. The jetting voltage and vacuum level were found to have a significant effect whereas the jetting frequency did not. Instabilities occurred in the form of individual deviating jet trajectory and also jet array failures. These were found to be initiated by air motion when using inappropriate jetting voltage resulting in incorrect jet trajectory. A combination of incorrect jetting voltage and vacuum level led to air bubble entrapment during jetting and, therefore, rapid failure of the jets. Analysis of jet array instability led to a stable process window for further stages of the research on the additive inkjet manufacturing process development.

Keywords Jettability · Jetting stability · Inkjet printing · Nylon 6 · Additive manufacturing

S. Fathi (✉) · P. Dickens · R. Hague
Additive Manufacturing Research Group,
Wolfson School of Mechanical and Manufacturing Engineering,
Loughborough University,
Loughborough, UK
e-mail: Saeed.Fathi@gmail.com

1 Introduction

1.1 Additive manufacturing

The concept of adding layers to manufacture parts was first introduced as rapid prototyping and has been in use to date for design prototypes. Progress in the additive layer techniques and the consequent increase in the functionality of parts resulted in the concept of rapid manufacturing [1]. Most recently, the term "additive manufacturing" was recognised by the American Society for Testing and Materials to standardise terminologies commonly used for different varieties of additive approaches [2].

Several layer fabrication techniques have been developed which have been categorised into liquid-based, powder-based and solid-based processes depending on the state of the material being processed during layer fabrication [1]. Examples are stereolithography, selective laser sintering and fused deposition modelling. Additive manufacturing processes are capable of producing net-shaped parts with great complexity due to their digital and additive layer capabilities. However, increasing the functionality of manufactured parts has been the subject of ongoing research. This has resulted in various technologies to process materials with higher functionality and enhanced process resolution which has also been the subject of this research work.

1.2 Inkjet technology

There has been rapid growth in employing inkjet printing for different non-graphical applications as the technology can deposit a wide range of materials on almost every substrate in a precise and controlled manner [3]. In addition, the digital nature of inkjet printing gives it an

advantage as information can be flexibly chosen from a computer for printing. Reproducibility is another advantage of inkjet printing as fault recognition and quality monitoring is easy to achieve in this type of printing [4]. This has resulted in the technology being used as a manufacturing tool in a wide range of applications including printed electronics, additive manufacturing and bioprinting [5–7].

Inkjet technology has been classified into two main techniques based on the jetting head used: continuous mode and drop-on-demand (DoD) mode. Detailed information on these modes can be found in the literature [4, 6, 8].

A train of droplets is made in continuous mode inkjet printing by pressurising the liquid through a feeding system and then vibrating a piezoelectric element inside the printhead. In a DoD mode inkjet head, a voltage signal is sent to a transducer that forces liquid material through a nozzle and a droplet is generated to hit the substrate when needed. Several actuation systems have been developed for DoD mode printing in which the thermal and piezoelectric systems are the most widely used [4]. Thermal actuation systems are mainly limited to water-based inks whereas a wide range of materials can be used with piezoelectric inkjet systems which enable the technology to be used as a manufacturing tool.

1.3 Inkjet-based additive manufacturing

Inkjet technology was first used in additive manufacturing in the early 1990s, resulting in commercialisation of the three-dimensional printing process by Soligen in 1993 [9]. The concept though was to deposit a binder solution to consolidate a powder bed. Early research on the use of inkjet technology to deposit the build material in an additive manufacturing approach was undertaken at MIT with printing 3D wax structures [10]. The first commercialisation of the concept was the *ModelMaker* process by Solidscape which was introduced in 1994. 3D Systems developed its wax 3D printing-based process, *Multi-Jet Modeller*, in 1997 which was later replaced by the *ThermoJet* system which had a better printhead technology for a faster process [9].

Additive manufacturing processes were developed based on printing photopolymer resins where an ultraviolet (UV) light could cure and solidify the deposited pattern. The first commercialisation of such a technique was introduced with *PolyJet* technology of Objet Geometries in 2001 [11]. The process could print two different photopolymer resins (as build and support materials) followed by a UV light scanner to solidify the layers in an additive manner. 3D Systems also introduced its first photopolymer-based 3D printing system, *InVision*, in 2003, which used wax as the support material [11].

Considering the fluid property restrictions, the research on jetting of materials is impressive and they have been printed for different applications. In the additive manufacturing approach, waxes have been used as vehicles in printing colloidal suspensions [12]. The process required a drying stage for each layer, and solvent was evaporated by either hot air or by a hot substrate. This requirement limits the process in terms of fabrication speed as well as surface finish. However, printing of thin features (of about 50 μm thick) and multi-graded ceramic composition structures was successfully achieved [13]. In inkjet additive manufacturing with metals, the Precision Droplet-Based Net Form Manufacturing process was developed by Orme to deposit molten aluminium via continuous mode jetting [14]. Research on jetting of metals for additive applications is still ongoing despite the restriction of jetting systems on elevated temperatures. Although a high jetting temperature of 1,200°C was achieved, a frequency higher than 10 Hz could not be obtained [15].

Most polymers are too viscous in their liquid state to jet due to their entangled long molecular chains. However, they can be jetted as a dilute solution or a colloidal dispersion [3, 16]. The idea of printing multiple reactive epoxy-based materials via separate printheads was first published as a patent by Johnson et al. [17]. Later, Elsner et al. [18] of Voxeljet Technology GmbH filed a similar patent on the concept and reported the printing of lines and multiple layers with this approach. The concept was developed for 3D printing of epoxy-based materials which still has the limitation of low mechanical properties for functional applications.

There is no known research which involves the use of anionic polymerisation of caprolactam as a part of an inkjet manufacturing technique. Additive manufacturing processes are mainly dominated by other grades of nylons such as nylon 11 and nylon 12 using the powder-based SLS process [11].

1.4 Research motivation and objectives

With jetting techniques to manufacture plastic parts, there is still the main limitation regarding their material properties. There is a need for an additive technique to produce parts from a functional polymer with high resolution and good surface finish. There are a number of reactive materials which could be jetted to give a functional polymer. The novelty in this work is using inkjet technology to manufacture nylon 6, which is one of the most widely used engineering plastics. However, nylon 6 in the melt state has such a high viscosity that it cannot be jetted. As it can be polymerised from mixtures of low viscosity caprolactam at elevated temperatures, the novel idea of "Inkjet Printing of Nylon Parts" was initiated at Loughborough University as a possible approach.

The polymerisation concept would be similar to the cast nylon process but instead of premixing the two reactive

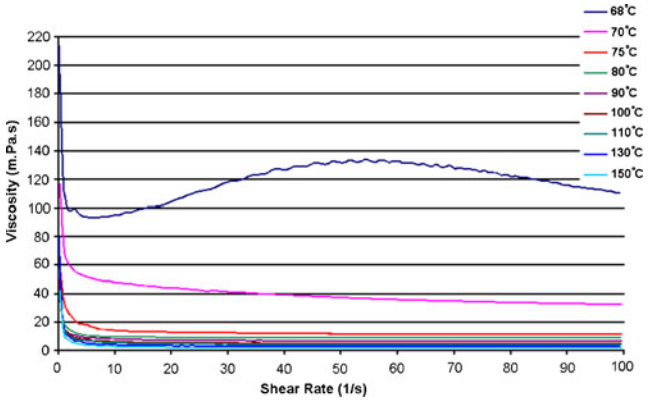

Fig. 1 Viscosity versus shear rate at different temperatures for molten caprolactam [20]

compounds, consisting of caprolactam and activator as *A* and catalyst as *B*, and injecting them into a heated mould at elevated temperatures, they could be deposited via inkjet printing. By depositing a layer of the two reactive mixtures on top of each other, the two mixtures were expected to mix and start the reaction under appropriate thermal and environmental conditions. This could produce nylon 6 as a solid layer before fabricating the next layer in an additive approach. Then, it would be possible to produce solid nylon parts with fine resolution and with acceptable build speed.

The commercial reactive mixtures for casting of nylon 6 are dominated by caprolactam at over 98% (volumetric). There was no evidence that caprolactam and these mixtures had been jetted before. Therefore, the first stage of the research was to investigate the jettability and jetting stability of molten caprolactam. It was necessary to determine the process parameter window for stable jetting. Other reactive materials could be jetted but confidentiality issues restrict further discussion on this.

2 Material and experimental procedure

2.1 Jetting material

Caprolactam (produced by Sigma-Aldrich GmbH) was provided as granules in sealed containers. It is white in the solid state but melts at 68°C in atmosphere and is colourless when molten [19]. The physical properties of caprolactam were considered as the starting point to determine the appropriate printhead and the design of the experimental setup.

The dynamic viscosity of molten caprolactam was measured over a range of temperatures [20]. Figure 1 shows the dynamic viscosity of caprolactam. It decreases rapidly with an increase in temperature. Therefore, with the high shear rates of jetting in the order of 10^4 [16], the caprolactam had a viscosity below 10 mPa s at temperatures higher than 75°C.

2.2 Experimental setup

2.2.1 Printhead

From the physical properties of the molten caprolactam and reviewing the available jetting technologies, it was expected that an industrial available printhead could be employed in the jetting system if an operating temperature above 75°C could be tolerated. A Xaar 126 piezoelectric DoD printhead was provided by Xaar Plc. (Cambridge, UK) for this research. With 126 nozzles (50 μm diameter) and 137 μm spacing, in an array of 17.2 mm width, the printhead was capable of jetting with a maximum frequency of 5.2 kHz.

The printhead could jet non-aqueous fluids with a viscosity between 8 to 13 mPa s, and its nozzle plate material had a surface tension of 40 mN/m (reported by the manufacturer). Operating temperatures of a maximum of 85°C could be used with the printhead. However, from the physical properties of the molten caprolactam, a jetting temperature of 80°C seemed to be reasonable as the viscosity at this temperature would be low enough. The surface tension of molten caprolactam, measured by pendent drop method (OCR 20 by DataPhysics Instruments GmbH), was found to be 34.9±0.3 mN/m at 80°C. Therefore, the nozzle plate would be wet by the molten caprolactam.

Operation of the printhead was undertaken through a controller known as a XUSB (by the manufacturer). The XUSB was powered by a power supply unit and controlled by software (XUSB software from Xaar Plc) on a windows based computer. A head personality card transferred the signals generated from the XUSB to the printhead. A single nozzle or an array of nozzles could

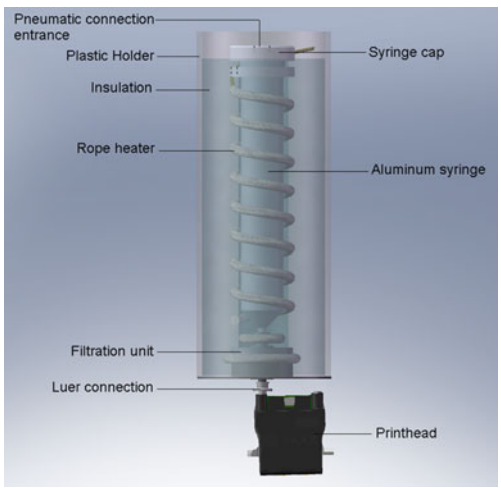

Fig. 2 Melt supply unit with luer connection joined to the printhead

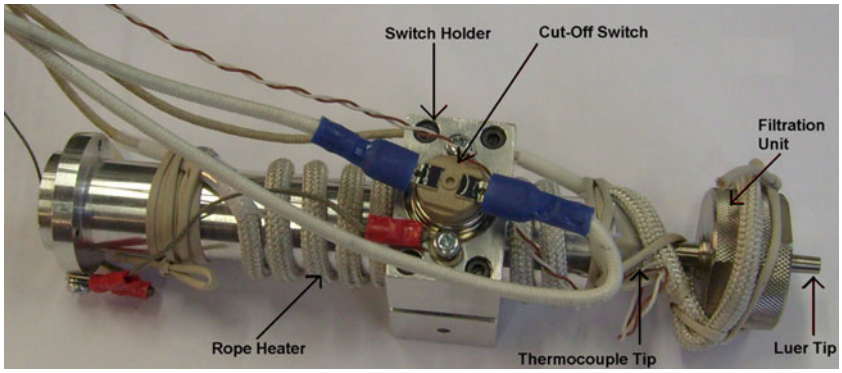

Fig. 3 Contents of the melt supply unit

be actuated by the software and be operated continuously for the jet stability study.

2.2.2 Printhead-caprolactam compatibility

The nozzle plate of the printhead was made from a heat resistant polyimide thin film. However, any change in the nozzle geometry could cause inconsistency in droplet separation from the nozzle plate and consequent problems such as droplet placement inaccuracy, therefore, it was important to know if the thin film swelled in the presence of caprolactam.

Six samples of the film (10×10 mm; supplied from Xaar plc) were immersed in separate glass tubes filled with molten caprolactam and placed in an oven at 90°C. Samples were removed from the oven after 1, 3, 8, 24, 64 and 104 h and then washed with water to remove caprolactam from the surface. After drying, each sample was observed under an optical microscope to detect any change on the surface and the edges. No geometrical and dimensional changes were found from swelling or surface deterioration in all samples. This showed that molten caprolactam would not affect the nozzles in continuous operation and, therefore, a jetting assembly was developed based on the chosen printhead.

2.2.3 Jetting assembly

The jetting assembly was the main part of the experimental setup and the thermal and fluidic control over the melt was key for a consistent and reliable supply for jetting. It consisted of a melt supply unit with thermal and pneumatic control, printhead with heaters, mount plate, fixtures and tubing.

Figure 2 shows the melt supply unit attached to the printhead. It consisted of an aluminium syringe with a 25-ml capacity, a flexible rope heater and a filtration unit attached to the syringe with a luer-type connection. The rope heater was insulated with cotton wool in a cylindrical holder. The connection on top of the syringe cap, as shown in Fig. 2, allowed a pneumatic tube to provide pressure or a vacuum for melt flow control, and so the cap was sealed to the syringe by an O-ring. Figure 3 shows the contents of the unit. Thermal control of the rope heater was achieved via a controller and a T-type thermocouple attached to the syringe at its conical end. The unit was also equipped with a cut-off switch attached to the syringe to cut the main power supply in case an unpredicted fault in the heating system occurred and the temperature rose above 100°C.

The filtration unit was to stop contamination entering the printhead which would otherwise clog the nozzles and diminish the jetting consistency and subsequent deposition reliability. It consisted of a metallic holder and a 25-mm diameter filter membrane with 5 μm pore size (Mitex Membrane Filter, LCWP02500, from Millipore Corp.).

The printhead was heated by two resistors (HS25, 25 W, from Arcol UK Ltd.) attached via two aluminium holders. A T-type thermocouple (RS Components Ltd.) embedded inside the holders near the printhead's nozzle plate was used to feedback the temperature for resistor control. The printhead with heaters was fixed to an aluminium plate, and then the melt supply unit was connected on top of it via a short plastic luer connection,

2.2.4 Thermal management in the jetting assembly

Four controlling channels were used for thermal management of the jetting assemblies by a seven-channel controller

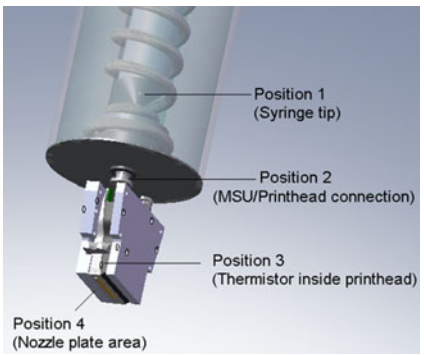

Fig. 4 Temperature reading positions in the jetting assembly

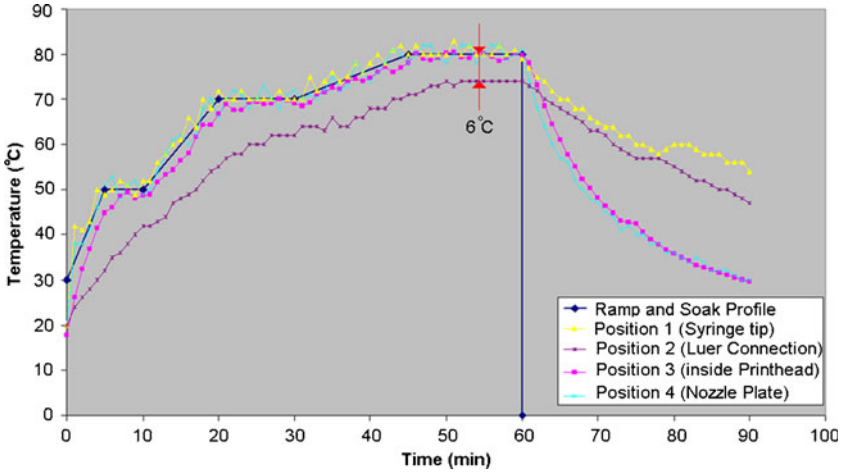

Fig. 5 Thermal behaviour of jetting assembly with the set ramp and soak temperature profile

(CN1507-TC1 by Omega Engineering Inc.). The feedback was via the T-type thermocouples installed in different positions of the assemblies. A thermistor was also embedded inside the printhead (by the manufacturer). Figure 4 shows the positions for the temperature measurements. Position 1 monitored the temperature at the syringe nozzle which was used to control the power given to the rope heater. In position 2, the thermocouple was attached to the exterior of the plastic luer connection joining the melt supply unit to the printhead. With no heating source allocated for this location, a short connection was key for a safe (hot) delivery of the melt mixture to the printhead, otherwise it could freeze and block the melt supply. The temperature inside the printhead could be read via the thermistor in position 3. The XUSB software used the temperature reading of position 3 for adjusting the voltage signals to the printhead. Varying the temperature could vary the melt viscosity, therefore, the amplitude of the voltage signal was adjusted automatically by the software to keep the jetting conditions set to the melt viscosity. In position 4, the thermocouple, embedded inside the aluminium resistor holder at about 2 mm from the nozzle plate (for controlling the resistors heating the printhead), controlled the nozzle plate temperature.

The thermal behaviour of the jetting assembly was monitored as shown in Fig. 5. All the heaters were switched off after 60 min. Position 2 had a temperature difference of 6°C from the set temperature of 80°C which showed the connection was short enough for the melt not to become frozen during the supply to the printhead.

2.2.5 Jet stability monitoring

A digital microscope camera (Dino Lite AM211 from ANMO Electronics Corp.) was used for monitoring the nozzle plate during jetting trials. It recorded the jet array behaviour when varying different parameters. In addition, the setup was equipped with a high-speed camera (FASTCAM APX-RS from Photron Inc.) with a long lens (12× Zoom from Navitar Inc.) in combination with an intensive light source (ELSV-60 from Everest VIT) placed opposite to the camera lens for backlight imaging. The camera was set at an imaging rate of 10,000 frames per second to capture the instabilities of a single jet.

2.3 Melt supply for jetting

Caprolactam was cast into an aluminium mould to form solid cartridges to fit into the syringe of the melt supply unit. The heating system of the jetting assembly set at 80°C could melt the inserted cartridge. A pneumatic system was developed to supply the printhead with the molten caprolactam through the filtration unit. An in-line venturi-type vacuum generator (GV2 from Vuototecnica Srl)

Table 1 Experiments undertaken for jet stability study of molten caprolactam

Set	Experiments objective	Jetting status	Voltage (V)		Frequency (kHz)		Vacuum (mbar)	
			Range	Increment	Range	Increment	Range	Increment
1	Meniscus control	No jetting	–	–	–	–	0~20	5
2	Jet stability	Jetting	10.0~20.0	2.5	1~5	1	15, 25	–
3	Jet array stability	Jetting	15.0~25.0	5.0	5	–	5~35	10
4	Air ingestion	Jetting	12.0~26.0	2.0	5	–	10~50	10

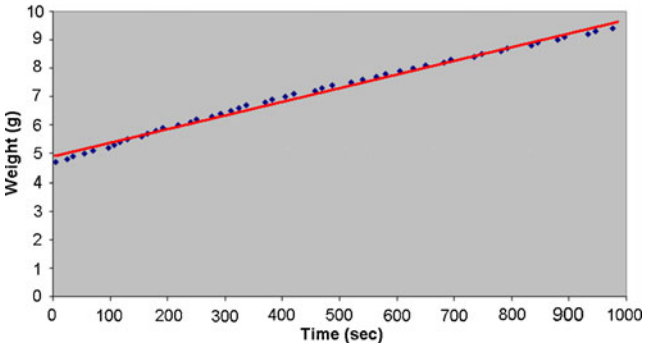

Fig. 6 Molten caprolactam flow due to the head pressure from the melt supply level in the jetting assembly (after initiation by a pressure signal)

supplied a vacuum by exhausting pressurised air. Both pressure and vacuum were regulated for the melt flow control by a digital manometer (FCO16 from Furness Controls Ltd.) working with 1 mbar resolution.

The pneumatic pressure in the jetting assembly was to feed the printhead with melt. As soon as dripping of the melt from the printhead was observed, a vacuum was applied to control the meniscus on the nozzles. The nozzle plate was monitored with the digital microscope camera to observe the flow of melt through the printhead nozzles. The pressure, required to fill the printhead and obtain dripping of melt through the nozzles, and also the vacuum, required to stop dripping and control the meniscus shape on the nozzle plate for jetting trials, were monitored. The melt flow rate was also measured during dripping of the melt. A beaker under the printhead collected the dripping melt and was weighed in situ by a digital scale (PW01 by Technico). This was undertaken in two situations, (1) when only the head pressure (gravity) of the melt was in place which could provide up to 15 mbar with the maximum level of melt (25 ml) in the supply unit and (2) when a pressure was applied.

2.4 Process parameters and trials for jetting

The variables for jetting were the melt temperature, the voltage signal for droplet generation, and the vacuum level. The melt temperature was set at 80°C in the jetting assembly. For the voltage signal, the amplitude and frequency could be varied whereas the waveform and pulse width of the actuation signal were fixed by the printhead manufacturer. The pulse amplitude and the signal frequency could be varied within 0 to 40.0 V and 0 to 5.2 kHz, respectively. The vacuum level which affected the meniscus shape and, therefore, the droplet formation, was varied from 5 to 50 mbar.

Table 1 lists the sets of experiments undertaken for jetting of molten caprolactam. All the trials were repeated three times and for at least 10 s each. Set 1 was to find the appropriate vacuum level which could control the melt flow and the melt meniscus on the nozzle.

Set 2 was to investigate if a stable jet could be developed when varying voltage and frequency. This was with two vacuum levels. It was found that frequency did not affect the jet stability and the chosen voltage increments did not make a visible change for trials with 15.0 V and over. Therefore, investigations continued with a new set of experiments in set 3, where jetting frequency was fixed at 5 kHz and voltage increments increased to 5.0 V. In this set of experiments, the vacuum level was varied over a wider range to observe any significant effect on the jet array stability. At higher vacuum levels, with high voltage, jet failure was observed in the jet array by air ingestion. Therefore, a new set of experiments (set 4) was undertaken to investigate the effect of voltage and vacuum level on the jet failure especially at high values. A finer voltage increment and a wider range of vacuum level were used to observe the stability behaviour.

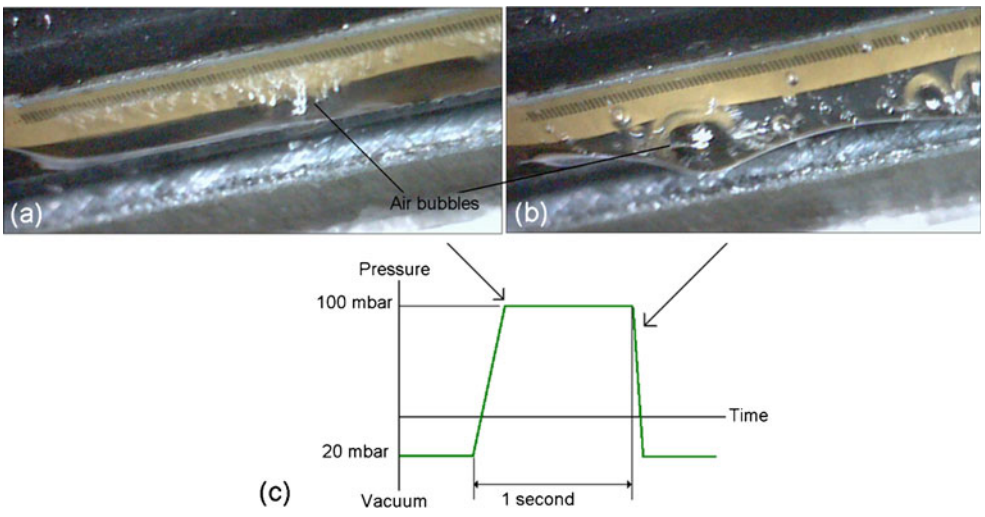

Fig. 7 Air bubbles trapped in the printhead revealed by purging of the molten caprolactam: **a** start of the pressure signal, **b** end of the pressure signal, and **c** the pneumatic purging signal

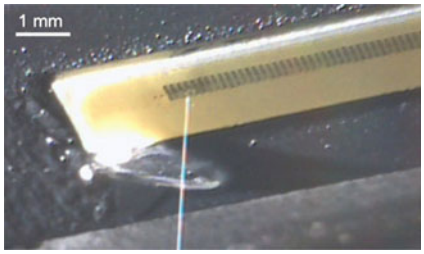

Fig. 8 Single jet of caprolactam (17.5 V, 4 kHz, 15 mbar, set 2)

3 Results and discussions

3.1 Melt supply behaviour

The molten caprolactam did not initially fill the printhead under gravity as no melt was observed on the nozzle plate. This could have been due to the resistance of the melt to flow through the pores of the filter membrane. Therefore, an initial pneumatic pressure of up to 100 mbar was required. This filled the printhead and provided dripping of the melt via the nozzles. After removing the pressure though, the dripping continued at a lower rate. The flow rate due to the head pressure after initiation was found to be consistent at about 0.3 g/min (or about 0.3 ml/min) as Fig. 6 shows. A vacuum of about 10 mbar could stop the dripping and retract the excess melt on the nozzle plate into the printhead. For the jetting trial, the nozzle plate was then cleaned with a lint-free cloth in order to remove any contamination within the excess melt on the nozzle plate. Due to the wettability of the molten caprolactam, a thin layer of melt was left on the nozzle plate after the meniscus retraction by the applied vacuum.

In some trials, air bubbles were trapped inside the printhead when supplying molten caprolactam as Fig. 7 shows. These images were taken at the start and end of a pressure signal of about 100 mbar amplitude. Air could be trapped when inserting the solid cartridge and could affect the supply behaviour of the melt. Due to the micro-size channels of the printhead, there could also be some air bubbles trapped and not removed by the pressure purging. A bleeding tube was used to ensure the removal of the trapped air from the melt supply before the jetting trials.

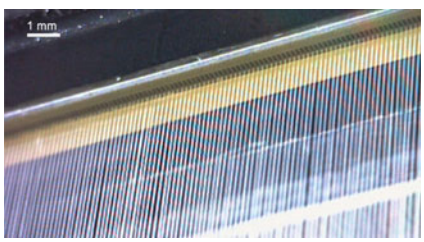

Fig. 9 Jet array of melt caprolactam (17.5 V, 5 kHz, 25 mbar, set 2)

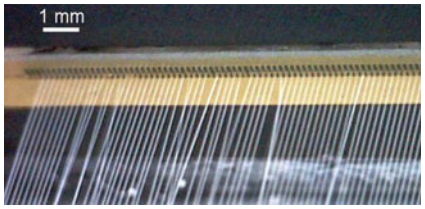

Fig. 10 Jet instabilities during trials with molten caprolactam

The tube was connected to the printhead ink outlet via a luer connection.

3.2 Jet stability observation

One of the main requirements was to investigate whether molten caprolactam could be jetted with a normal graphics industry printhead. This was confirmed initially by triggering one nozzle of the printhead in set 2 of the experiments. A single jet of molten caprolactam was achieved as seen in Fig. 8 with voltage, frequency and vacuum level set at 17.5 V, 4 kHz, and 15 mbar, respectively. Multiple jets of caprolactam were also produced as seen in Fig. 9 (with 126 jets) with 17.5 V, 5 kHz, and 25 mbar, and all jets were stable. However, within the trials some instability occurred especially when jetting an array as seen in Fig. 10. As the instability could have originated externally by contamination or air motion, the trials with instability were repeated after a purging period (for a further three times). This was to check if the instability occurred due to improper setting of parameters.

Figure 11 shows the results for set 2 experiments. Similar stability behaviour was seen for both single and multiple jets in this set. Decreasing jetting voltage, however, resulted in instability and no jet was developed with a low voltage of 10.0 V. The effect of jetting voltage and vacuum level on the jet stability is shown in Fig. 12

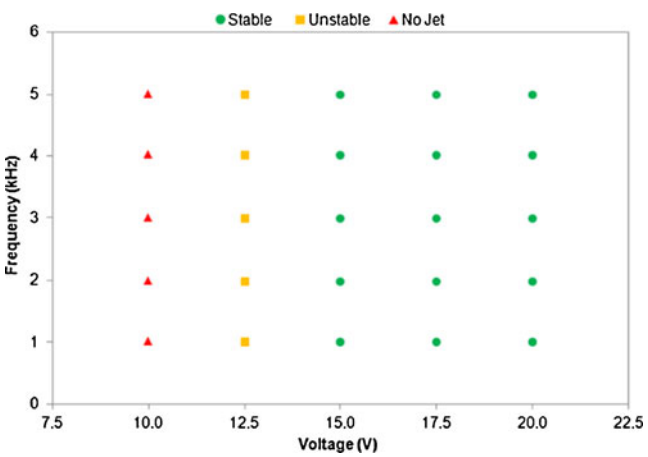

Fig. 11 Stability of single jet and jet array in set 2 (15 and 25 mbar)

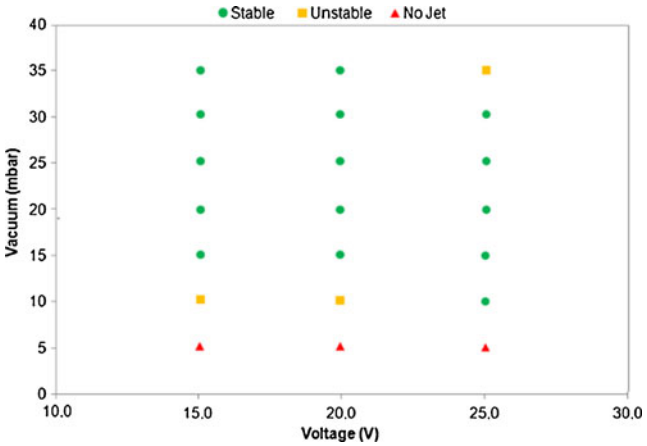

Fig. 12 Stability of single jet and jet array in set 3 (5 kHz)

which presents results for set 3. No jet occurred with 5 mbar vacuum level and instability occurred when using low jetting voltage and a 10-mbar vacuum. Also, a combination of high values of these two parameters resulted in unstable jets. Results from set 4, shown in Fig. 13, give a better understanding of the instability behaviour when varying voltage and vacuum levels. Some jets failed in the jet array with the vacuum set at 50 mbar at all jetting voltages at the very start of the trial. All the remaining jets failed within seconds which indicated a time-dependent phenomenon responsible for the jet failures.

3.3 Jet instabilities

Instabilities occurred in the form of individual jet trajectory which could lead to single jet failure and occasionally jet array failure where all jets in an array failed. In most cases, this started from a single jet failure. Figure 14b illustrates the instability types in individual jets. In Fig. 14a, the front and side view schematics of the jet array depict the types of

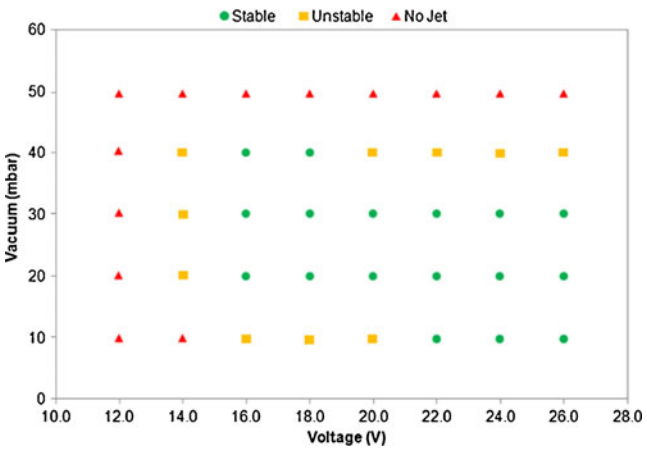

Fig. 13 Stability of single jet and jet array in set 4 (5 kHz)

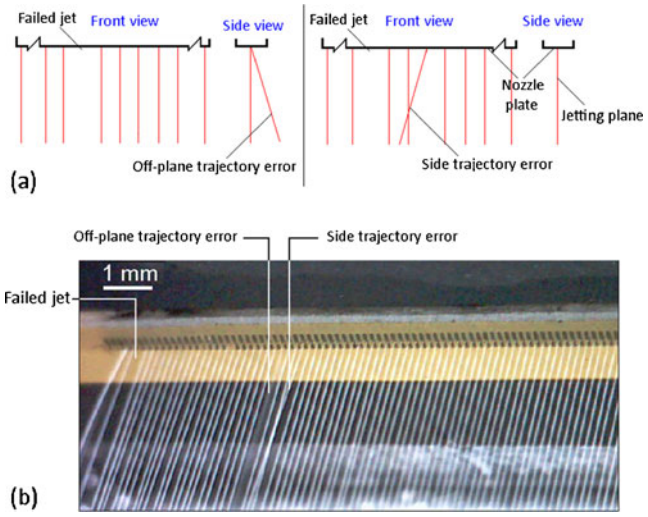

Fig. 14 Instabilities of individual jets in the jet array: **a** schematic and **b** actual situation (15.0 V, 5 kHz, 30 mbar)

instabilities, and Fig. 14b shows the actual situation. The jetting plane was considered as the plane normal to the nozzle plate passing through the line of jets. As a jet with an off-plane error did not reflect light the same as the others, it was easily recognised as in Fig. 14b. The side trajectory error was defined as still on the jetting plane but angled towards an adjacent jet. A failed jet is also shown in Fig. 14b.

With the start-up strategy, the risk of air entrapment in the melt supply was eliminated but there were still instabilities in individual jets or in the array of jets in some experiments. Jet instability was observed when the jetting voltage and vacuum level were low. No jet was produced for jetting voltages below 12.5 V and with vacuum levels as low as 5 mbar. In such a case, the pressure wave generated by the nozzle actuation inside the melt channel was dissipated when propagating towards the meniscus on the nozzle.

Figure 15 shows jet instability in an array which originated from the jetting parameters being set too low. However, as Fig. 15 shows, more jets exhibited instability with low jetting voltage (Fig. 15a) than with low vacuum level (Fig. 15b). Increasing the jetting voltage from 12.0 to 15.0 V increased the number of stable jets significantly despite the decrease of vacuum level from 20 to 10 mbar. This behaviour was repeatable within the trials which suggests jet stability was influenced by voltage more than vacuum level.

Droplets with less kinetic energy were generated with low jetting voltages or low vacuum levels due to the pressure wave dissipation in the meniscus oscillation. Therefore, air motion around the nozzle plate could affect the droplets and alter the jet trajectory. Although the jetting system was enclosed in a glove box to control the surrounding air motion, the

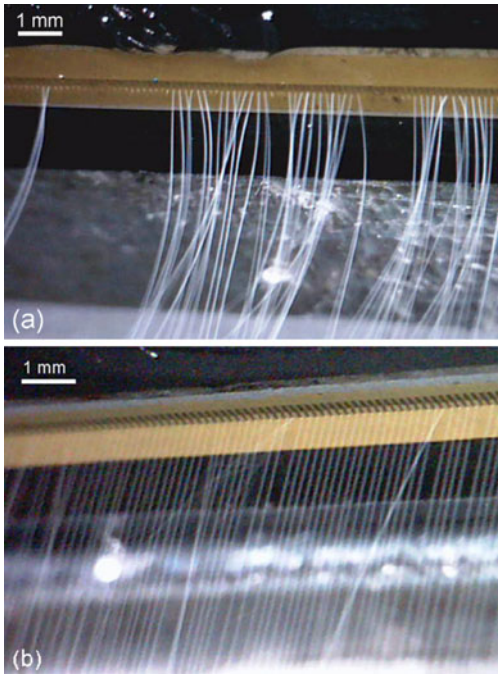

Fig. 15 Instability in jet array with **a** low jetting voltage (12.0 V, 5 kHz, 20 mbar) and **b** low vacuum level (15.0 V, 5 kHz, 10 mbar)

temperature gradient between the nozzle plate (kept at 80°C) and the jetting environment (around 20°C), could cause air motion due to heat convection.

With jetting voltages below 15.0 V with all vacuum levels or 20.0 V and vacuum levels equal to or below 10 mbar, a trajectory error occurred. The cause of the instability was the combination of low voltage and vacuum resulting in insufficient droplet kinetics. In such a situation, the jet trajectory error could lead to a jet failure. This situation was recorded by the high-speed camera as shown in Fig. 16. From the first ejected droplet in Fig. 16a, a trajectory error of 8° is seen. The trajectory error increased to 12° after 0.8 ms of jetting as seen in Fig. 16b and then to 45° after about 335 ms (Fig. 16c). This continued until the jet was parallel to the nozzle plate (Fig. 16d). When the droplets touched the nozzle plate, it led to failure of the jet after about 1 s. This shows how the individual jets could become unstable when using inadequate jetting voltage and vacuum level.

Figure 17 shows the above situation within a jet array. At t=0.1 s in Fig. 17a, a trajectory error occurred (J1). After a further 2 s (Fig. 17b), a trajectory error also occurred in three other jets (J2, J3 and J4). J2 failed at 2.5 s and failure of J3 occurred at 2.6 s. The bleeding through a failed jet could affect the wetting molten layer thickness locally affecting the adjacent nozzles droplet formation. The possibility of a jet failure could increase with contamination or air bubbles entrapped inside the nozzle. This could make a jet sensitive to bleeding from an adjacent nozzle and its consequent molten layer thickness variation.

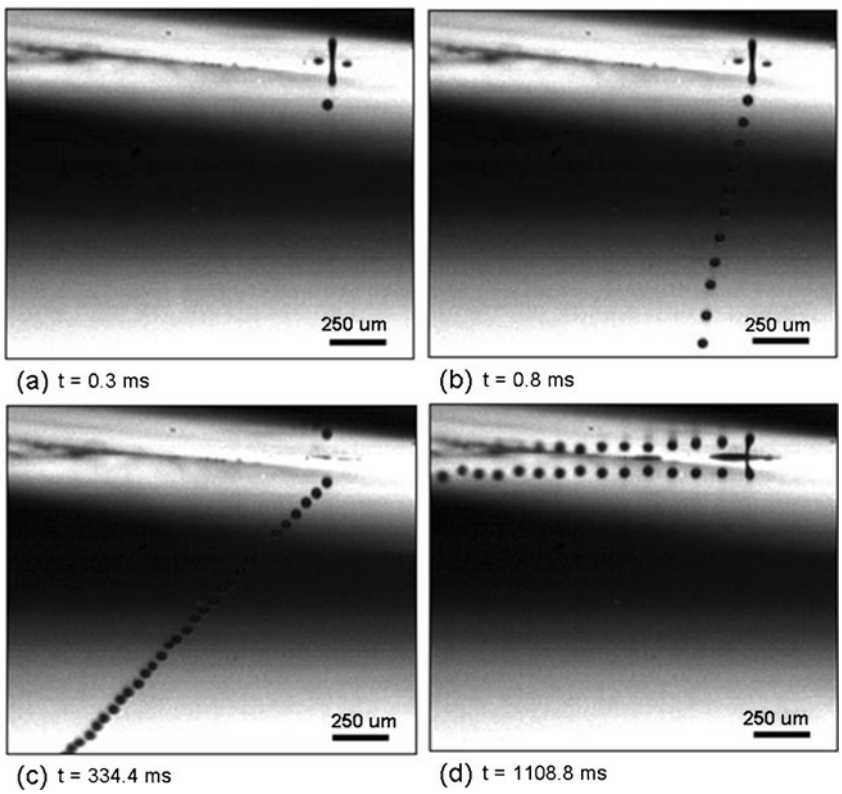

Fig. 16 Jet trajectory alteration by air motion in a trial with caprolactam using a low jetting voltage (13.0 V, 5 kHz, 25 mbar)

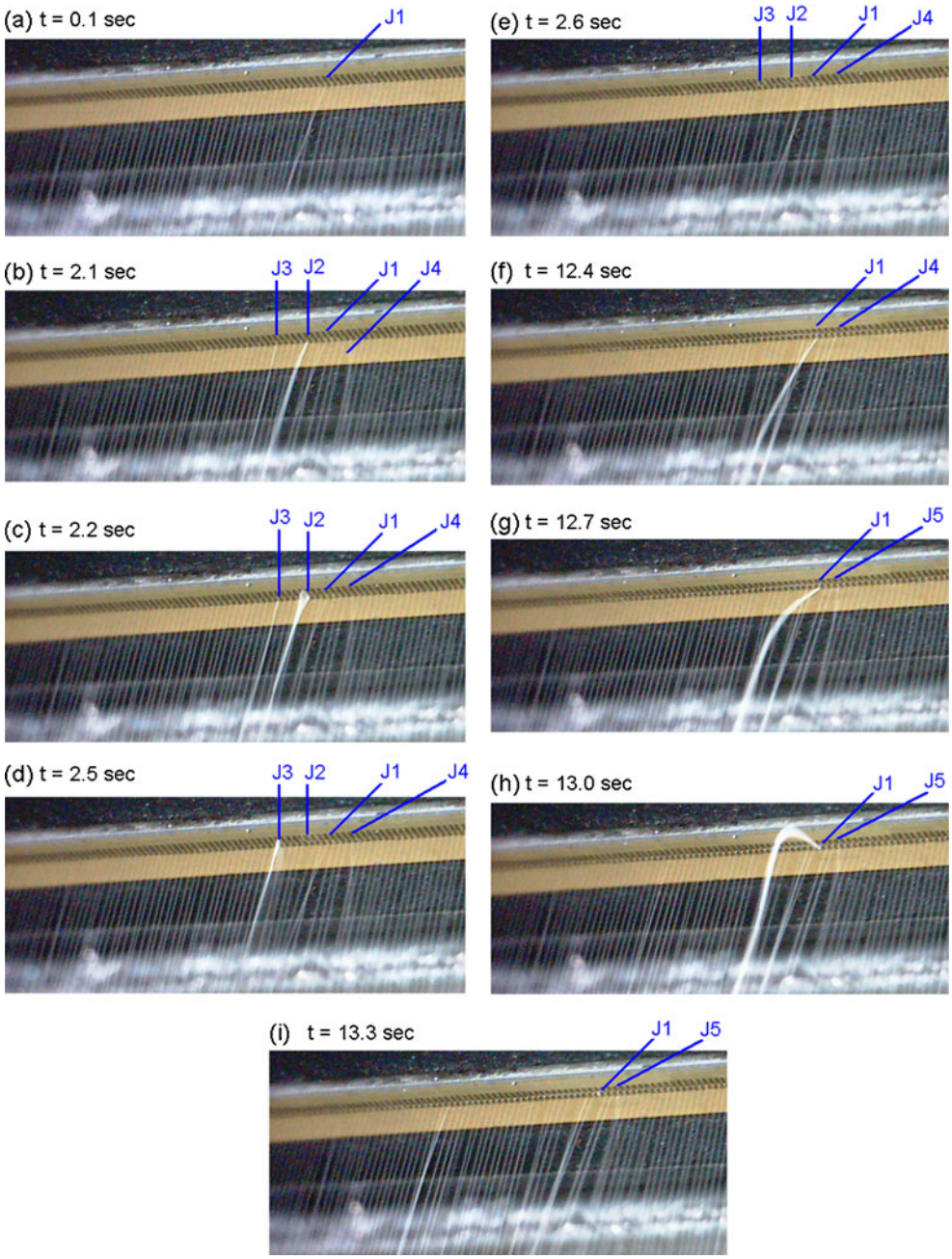

Fig. 17 Trajectory error developing to a jet failure (15.0 V, 5 kHz, 10 mbar)

Therefore, the failure of J3 in Fig. 17 could have been a result of bleeding from the nozzle of failed J2, where the jets between J2 and J3 could have less sensitivity to the bleeding.

The jet instability behaviour in an array was different in trials with low jetting parameters. A trajectory error can result in jet failure or be temporary as with J4 in Fig. 17b which started at t=2.1 s and re-stabilised at t=12.4 s when a trajectory error then occurred for its adjacent jet (J5). The error in the trajectory of J1 was constant until t=12.4 s where it then started to increase (from Fig. 17f–h) and finally caused failure of the jet (Fig. 17i). This transition from a

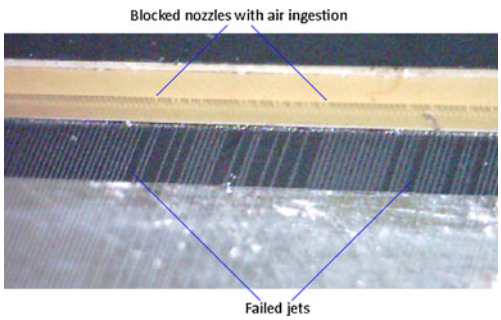

Fig. 18 Individual jet failure with high voltage and vacuum level (24.0 V, 5 kHz, 50 mbar)

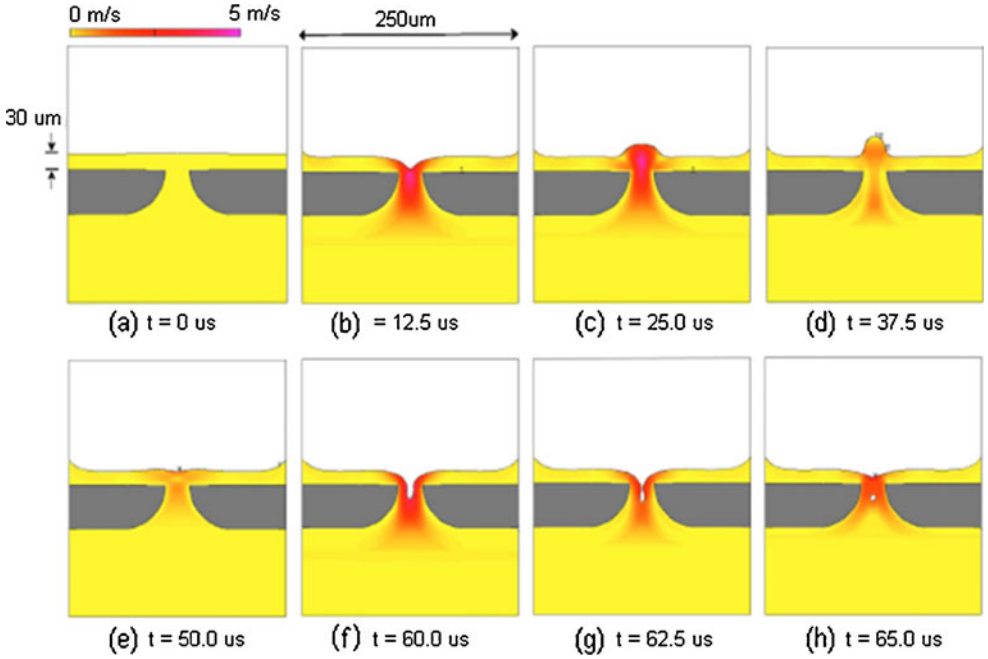

Fig. 19 Modelling of air ingestion during meniscus oscillation in a DoD inkjet printhead [21]

trajectory error to jet failure could be a slow process. In contrast, the failure of J2 occurred quickly (Fig. 17c). The failure of J1 after a period of constant trajectory could be a result of bleeding from the nozzles of failed jets (J2 and J3) which could change the wetting molten layer thickness locally.

Jet instability was also observed at high vacuum levels as seen in set 4. Individual nozzles failed during the trials as shown in Fig. 18 typically with a vacuum level at 50 mbar. When next applying a pressure signal to the nozzle plate, molten caprolactam was purged through all the nozzles. Air bubbles were found in the melt coming from the failed nozzles. Trials with the initial purging were repeated to ensure the removal of previous air entrapment. However, air bubbles were formed again as soon as the jetting trial started causing repeated nozzle blocking. In trials with jetting voltages and vacuum level equal or below 25.0 V and 30 mbar, no nozzle blocking by air bubbles was observed. However, when increasing the vacuum level, air entrapment occurred at lower jetting voltage than 25.0 V as seen in set 4. In such a case, with increasing voltage at high vacuum levels (higher than 40 mbar), the number of air bubbles extracted by pressure purging increased.

It was likely that air ingestion generated the air bubbles. The air ingestion was due to the meniscus oscillation while expelling a droplet. Upon droplet separation from the nozzle, the consequent suction of the melt meniscus into the nozzle by the printhead nozzle channel contraction could entrap an air bubble. A similar situation was reported by de Jong et al. [21] for a single nozzle jetting with a piezoelectric DoD printhead as shown in Fig. 19. After hundreds of droplets were expelled, repetition of the air ingestion process could increase the bubble size as shown schematically in Fig. 19. With a certain bubble size, the pressure wave (from the actuation) was dissipated in the entrapped air bubble and could not oscillate the meniscus adequately resulting in the jet failure.

3.4 Recommendations for stable jetting

Figure 20 gives a general guideline for setting the two parameters of voltage and vacuum in relation to each other for stable jetting of molten caprolactam. Jetting stability was sensitive to jetting voltage and vacuum level, whereas jetting frequency did not play a significant role. As a combination of high voltage and high vacuum level led to air ingestion and consequent nozzle blocking, it is recommended that at higher jetting voltage, the vacuum level is decreased and vice versa.

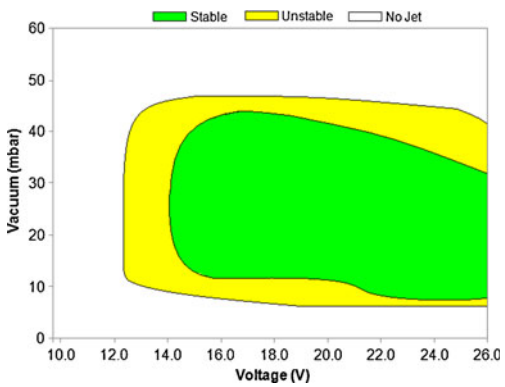

Fig. 20 Guideline jetting parameters for caprolactam at 80°C

4 Conclusions

It was demonstrated that supply of molten caprolactam at 80°C could be controlled for jetting with a printhead used in the graphics industry. A stable single jet and also successful trials with an array of 126 jets were performed and a processing window for stable jetting was recommended. Jetting frequency had no significant effect on the jetting stability. However, the jets were sensitive to the voltage and vacuum level. Too low or too high values of these parameters induced instability in the form of a trajectory error and in some cases jet failure. With too low jetting voltage and vacuum level, the pressure wave generated by the nozzle actuation, dissipated too much so that no droplet was formed or droplets had too low kinetics so that the air motion due to convection deviated the jet and resulted in the instability. With high vacuum levels, air ingestion occurred during nozzle actuation especially when accompanied with higher voltages and resulted in individual jet failures. Overall, the jetting voltage was found to have stronger influence on stable jetting than the vacuum level.

References

1. Hopkinson N, Hague RJM, Dickens PM (2006) Rapid manufacturing: an industrial revolution for the digital age. Wiley, West Sussex
2. ASTM (2009) ASTM WK24055—new terminology for additive manufacturing. Available at: http://www.astm.org/commit/committee/F42.htm. Accessed 22 September 2010
3. Calvert P (2001) Inkjet printing for materials and devices. Chem Mater 13:3299–3305. doi:10.1021/cm0101632
4. Le HP (1998) Progress and trends in inkjet printing technology. J Imaging Sci Technol 42:42–69
5. Mironov V, Reis N, Derby B (2006) Bioprinting: a beginning. Tissue Eng 12:631–634. doi:10.1089/ten.2006.12.631
6. Hon KKB, Li L, Hutchings IM (2008) Direct writing technology—advances and developments. CIRP Ann Manuf Technol 57:601–620. doi:10.1016/j.cirp.2008.09.006
7. Singh M, Haverinen HM, Dhagat P, Jabbour GE (2010) Inkjet printing: process and its applications. Adv Mater 22:673–685. doi:10.1002/adma.200901141
8. Pique A, Chrisey B (2002) Direct-write technologies for rapid prototyping applications. Academic, San Diego
9. Wohlers T (2007) Wohlers Report 2007. Wohlers Associates Inc., Colorado
10. Gao F, Sonin AA (1994) Precise deposition of molten microdrops: the physics of digital microfabrication. Proc R Soc Lond A 444:533–554. doi:10.1098/rspa.1994.0037
11. Gibson I, Rosen DW, Stucker B (2009) Additive manufacturing technologies: rapid prototyping to direct digital manufacturing. Springer, New York
12. Wang T, Hall D, Derby B (2004) Inkjet printing of wax-based PZT suspensions. Key Eng Mat 264–268:697–700. doi:10.4028/www.scientific.net/KEM.264-268
13. Lejeune M, Chartier T, Dossou-Yovo C, Noguera R (2009) Inkjet printing of ceramic micro-pillar arrays. J Eur Ceram Soc 29:905–911. doi:10.1016/j.jeurceramsoc.2008.07.040
14. Orme M (1991) On the genesis of droplet stream microspeed dispersions. Phys Fluids 3:2936–2947. doi:10.1063/1.857836
15. Xiang-hui Z, Le-hua Q, Hua H, Xiao-shan J, Yuan X (2010) Experimental research of pneumatic drop-on-demand high temperature droplet deposition for rapid prototyping. Key Eng Mat 419–420:405–408. doi:10.4028/www.scientific.net/KEM.419-420.405
16. de Gans BJ, Duineveld PC, Schubert US (2004) Inkjet printing of polymers: state of the art and future developments. Adv Mater 16:203–213. doi:10.1002/adma.200300385
17. Johnson DR, Kynaston-Pearson AW, Damarell WN (2003) Inkjet printer which deposits at least two fluids on a substrate such that the fluids react chemically to form a product thereon. US Patent GB2382798(A)
18. Elsner P, Dreher S, Ederer I, Voit B, Gudrun J, Stephan M (2010) Method and device for production of a three-dimensional article. US Patent 7767130
19. Ritz J, Fuchs H, Kieczka H, Moran WC (2002) Caprolactam: Ullmann's encyclopedia of industrial chemistry. Wiley, Weinheim. doi:10.1002/14356007.a05_031
20. Fouchal F, Dickens PM (2006) Anionic polymerisation of caprolactam for additive manufacturing application. Internal Report, Loughborough University, UK
21. de Jong J, de Bruin G, Reinten H, van den Berg M, Wijshoff H, Versluis M, Lohse D (2006) Air entrapment in piezo-driven inkjet printheads. J Acoust Soc Am 120:1257–1265. doi:10.1121/1.2216560